

Supporting Information

A new strategy of constructing covalently connected MOF@COF core-shell heterostructure for enhanced photocatalytic hydrogen evolution

Hong-Yu Zhang[†], Yan Yang[†], Chang-Cheng Li, Hong-Liang Tang, Feng-Ming Zhang*, Gui-Ling Zhang and Hong Yan*

Key Laboratory of Green Chemical Engineering and Technology of Heilongjiang Province, College of Material Science and Chemical Engineering, Harbin University of Science and Technology, No.4, Linyuan Road, Harbin 150040, P. R. China.

[†] These authors contributed equally to this work.

Experimental Section

Materials and General Methods. Except for the 1,3,5-triformylphloroglucinol (Tp) synthesized according to the literature method, all the chemical reagents and chemical solvents are directly purchased commercially without an additional purification process.¹ X-ray powder diffraction (XRD) patterns (Bruker D8 X-ray diffractometer), Fourier transform infrared (FT-IR) spectra (Spectrum 100) and thermogravimetric analyses (TGA) (SDTA851e) are used to study the structure and composition of synthetic materials. The texture properties of synthetic materials were observed by scanning electron microscopy (SEM) micrographs (Hitachi S-4800), and transmission electron microscopy (TEM) experiment (JEM-2100 electron microscope). The synthetic sample after soaking in acetone and vacuum drying at 120 °C for 12 hours

was passed through Micromeritics ASAP 2020 to evaluate the nitrogen adsorption of the material at 77 K. Optical properties were also studied by UV-vis diffuse reflectance spectroscopy (Lambda 35 spectrometer), photoluminescence spectrum (PL) (SPEX Fluorolog-3 spectrofluorometer with an excitation wavelength of 350 nm) and time-resolved PL of the samples were recorded with FLS1000 Photoluminescence Spectrometer under excitation of nanosecond flashlamp. The electrochemical impedance spectra (EIS), Mott-Schottky (M-S) plot and photocurrent-time (IT) profiles were measured on the CHI660E electrochemical workstation using a standard three-electrode system with the photocatalyst-coated ITO as the working electrode, Pt plate as the counter electrode, and a saturated calomel electrode as a reference electrode. The synthesized sample (2 mg), a mixture of 1 mL ethanol and 10 μ L Nafion was dripped onto the surface of the ITO glass electrode and dried until the working electrode. The 0.25 M Na_2SO_4 solution was used as the electrolyte solution. The light response signal of the sample was measured under 0.5 V chopped light with a 300 W xenon lamp with a 420 nm cut-off filter was used as the light source. The surface photovoltage spectroscopy (SPV) measurements of the samples were carried out with a home-built apparatus equipped with a lock-in amplifier (SR830) synchronized with a light chopper (SR540).

Synthesis of MOF-808: The zirconium oxychloride (0.32 g, 1 mmol) was sonicated in N,N-dimethylformamide (DMF, 20 mL) for 5 min, then formic acid (20 mL) was added and then sonicated for 5 min. 1,3,5-benzenetricarboxylic acid (0.21 g, 1 mmol) was added and stirred in an oil bath at 120 $^{\circ}\text{C}$ for 24 h, then cooled to room temperature

naturally, and the product MOF-808 was separated by centrifugation. After washing 3 times with dichloromethane and n-hexane, respectively, drying in an oven at 100 °C for 6 h, the product obtained is MOF-808.

Synthesis of amino functionalized MOF-808: The washed MOF-808 (0.2 g) was ultrasonically dispersed in DMF (10 mL), p-aminobenzoic acid (0.72 g, 5.2 mmol) was added and reacted at 60 °C for 48 h to obtain amino-functionalized MOF-808. The obtained product was washed three times with water and ethanol, respectively, then placed in an oven and dried at 100 °C for 12 h.

Synthesis of MOF-808@TpPa-1-COF: Add Tp, NH₂-MOF-808 and Pa to the vacuum tank according to the amount in Table S1, and then add the solvents 1, 4-dioxane (1.5 mL) and mesitylene (1.5 mL) and sonicate for 30 min. After sonication is completed, acetic acid (0.5 mL, 3 M) is added in sequence, and the mixture is uniformly mixed and subjected to three freeze-thaw degassing cycles. Put it in an oven and heat at 120 °C to react for 72 h, then cool to room temperature and filter to obtain the product, and wash the product with tetrahydrofuran. The resulting product was soaked in anhydrous acetone for 72 h, during which the acetone was changed 6 times. The obtained MOF-808@TpPa-1-COF was dried at 120 °C under vacuum for 12 h.

Table S1. Synthetic conditions of MOF-808@TpPa-1-COF in different proportions.

Weight ratio (MOF-808/TpPa-1-COF)	NH ₂ -MOF-808 (mg)	Tp (mg)	Pa (mg)
8/2	40	8	5.2
7/3	21	8	5.2
6/4	45	24	16
5/5	30	24	16
4/6	20	24	16
3/7	12.8	24	16

Photocatalytic hydrogen evolution: The photocatalytic activity on-line analysis system for hydrogen production by photolysis of water is tested in a buffer solvent system under vacuum conditions. During the test, a 300 W xenon lamp was used to simulate sunlight, and a 420 nm filter was used to ensure that the experimental light was visible light. For each experiment, weigh 10 mg of catalyst, 100 mg of sodium ascorbate in 50 mL of buffer solution, sonicated for 30 min, and then add 100 μ L of chloroplatinic acid hexahydrate. Before lighting, vacuum the system with an oil pump to ensure that there are no interference factors such as air in the system, and then use xenon lamp irradiation to reduce chloroplatinic acid to Pt and deposit on the surface of COFs. After turning off the vacuum pump, use gas chromatography (GC112A) to sample online once an hour, and calculate the photocatalytic hydrogen production from the standard curve to determine the photocatalytic hydrogen production activity. The apparent quantum efficiency (AQE) of hydrogen generation was determined using the same closed loop system under the illumination of a 300 W Xe lamp with optical filters (420, 450, 500, 550, 600 and 650 nm).

Apparent Quantum Efficiency (AQE) calculation process:

$$N = \frac{E\lambda}{hc}$$

AQE

$$= \frac{\text{the number of reacted electrons}}{\text{the number of incident photons}} \times 100\% = \frac{2 \times \text{the number of reacted electrons}}{\text{the number of incident photons}} \times 100\%$$

h is Plank constant = $6.62606957 \times 10^{-34}$ J·S

c is velocity of light = 2.99792458×10^8 m·S⁻¹

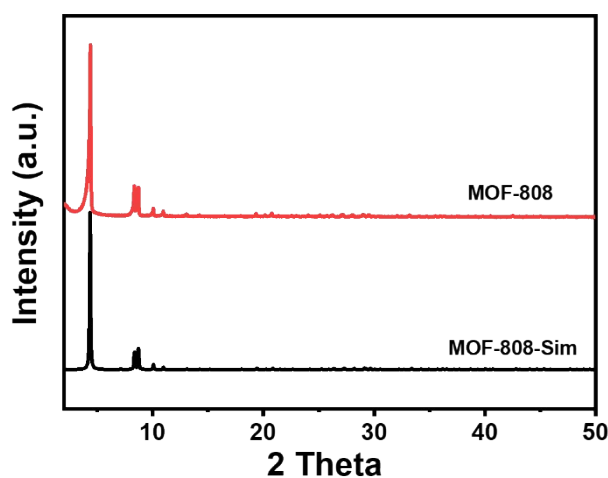


Fig. S1 The PXRD patterns of MOF-808.

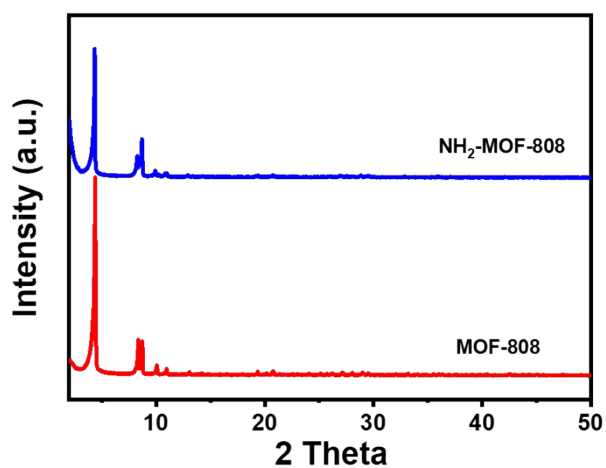


Fig. S2 The PXRD patterns of MOF-808 and NH₂-MOF-808.

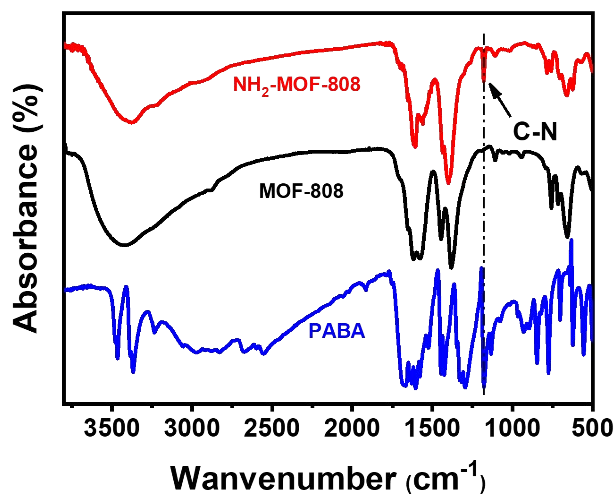


Fig. S3 The FT-IR spectrum of MOF-808, PABA and NH₂-MOF-808.

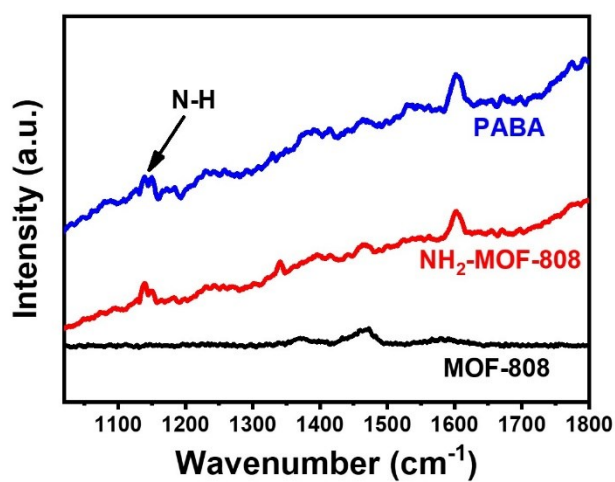


Fig. S4 The Raman spectrum of MOF-808, PABA and NH₂-MOF-808.

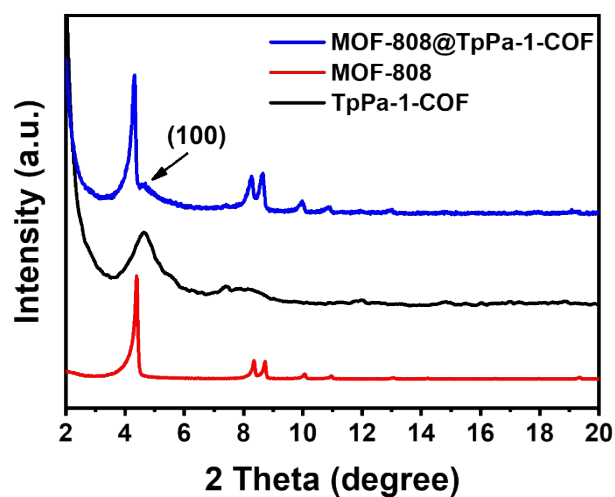


Fig. S5 Enlarging the PXRD patterns of MOF-808, TpPa-1-COF and MOF-808@TpPa-1-COF

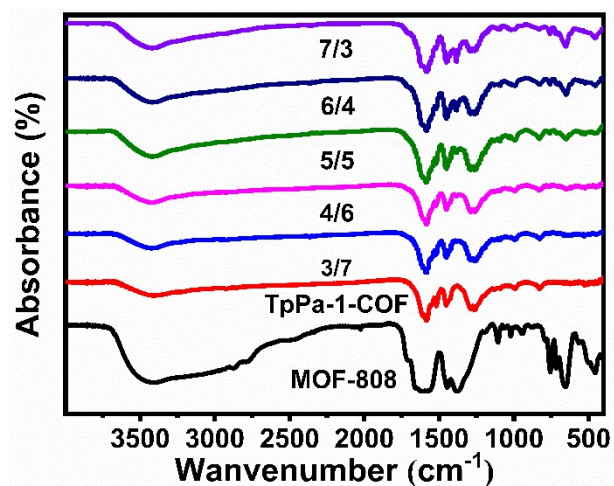


Fig. S6 The FT-IR spectra of MOF-808@TpPa-1-COF with different mass ratios.

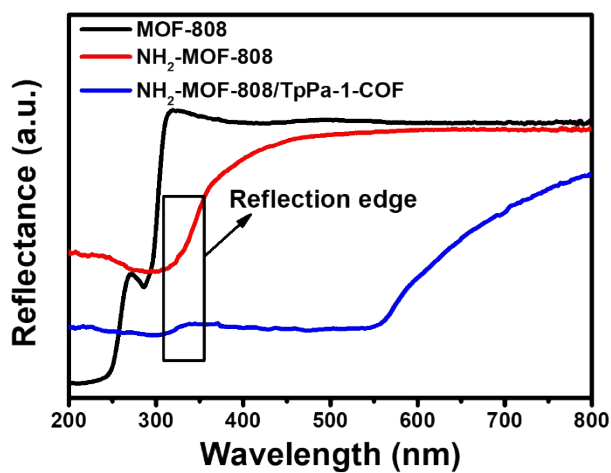


Fig. S7 The DRS spectra of MOF-808, NH₂-MOF-808 and NH₂-MOF-808/TpPa-1-COF (6/4).

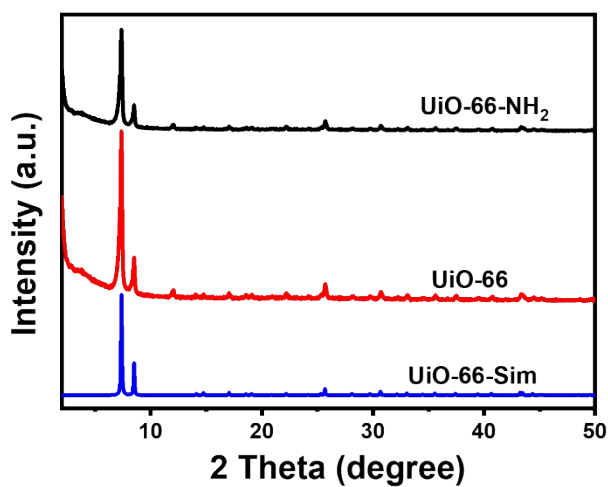


Fig. S8 The PXRD patterns of UiO-66 and UiO-66-NH₂

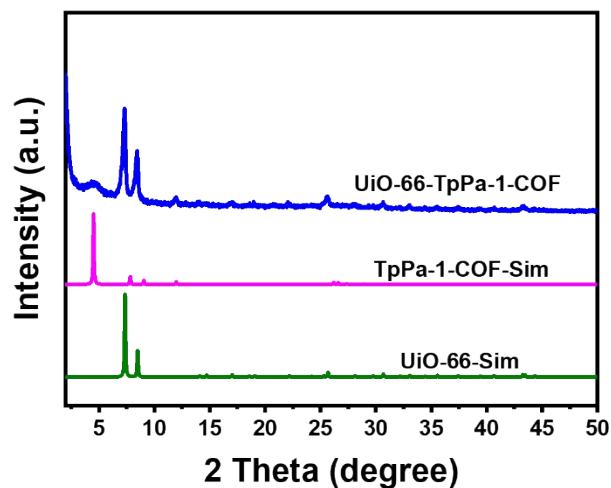


Fig. S9 The PXR D patterns of UiO-66-TpPa-1-COF.

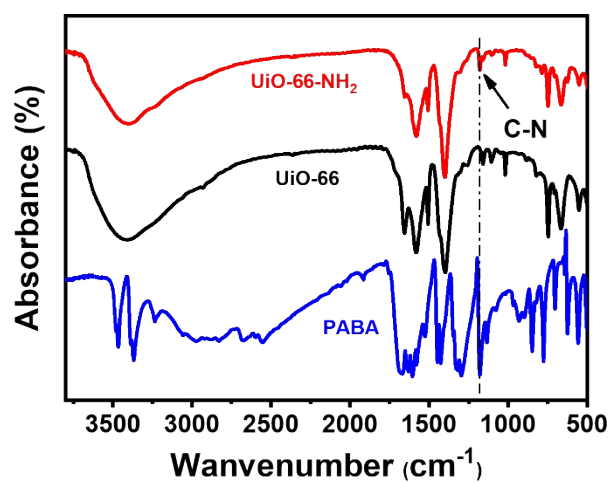


Fig. S10 The FT-IR spectra of PABA, UiO-66 and UiO-66-NH₂.

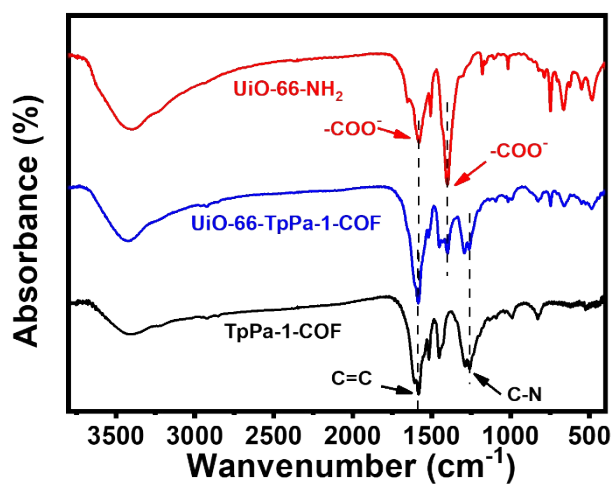


Fig. S11 The FT-IR spectra of UiO-66-NH₂, TpPa-1-COF and UiO-66-TpPa-1-COF.

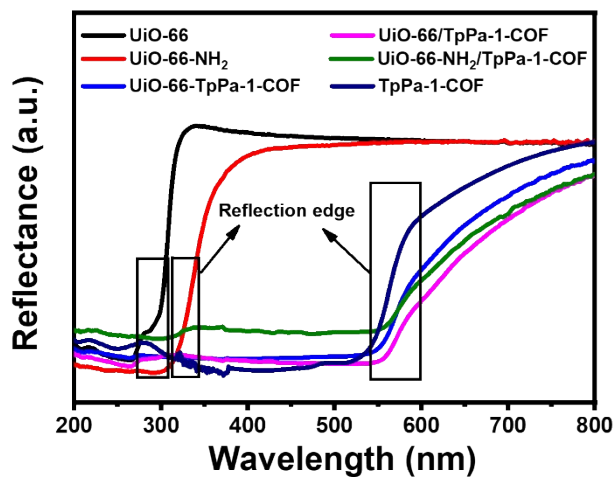


Fig. S12 The DRS spectra of UiO-66, UiO-66-NH₂, TpPa-1-COF, UiO-66/TpPa-1-COF, UiO-66-NH₂/TpPA-1-COF and UiO-66-TpPA-1-COF.

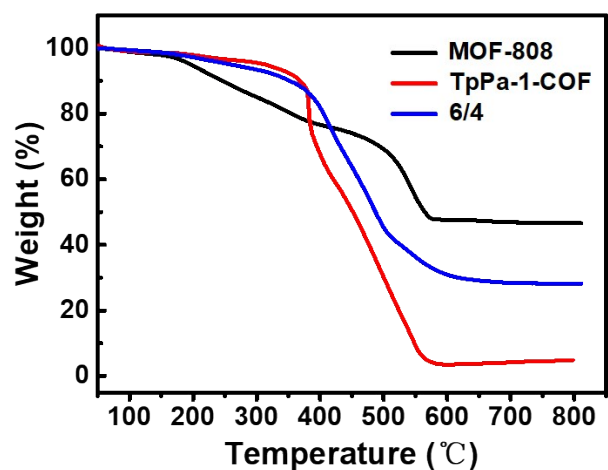


Fig. S13 The TGA curves of MOF-808, TpPa-1-COF and MOF-808@TpPa-1-COF (6:4).

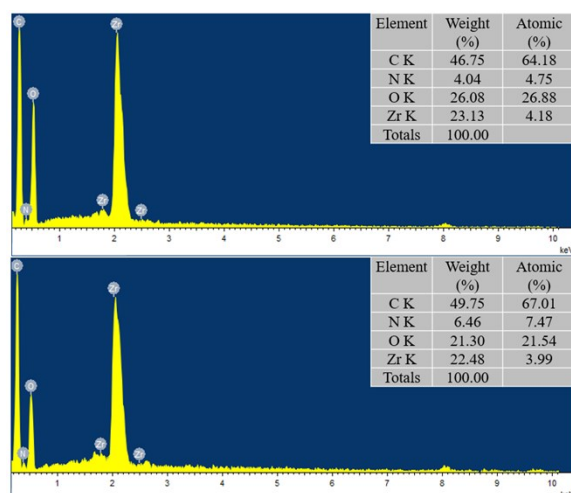


Fig. S14 EDS spectra of MOF-808@TpPa-1-COF (6:4) hybrid material.

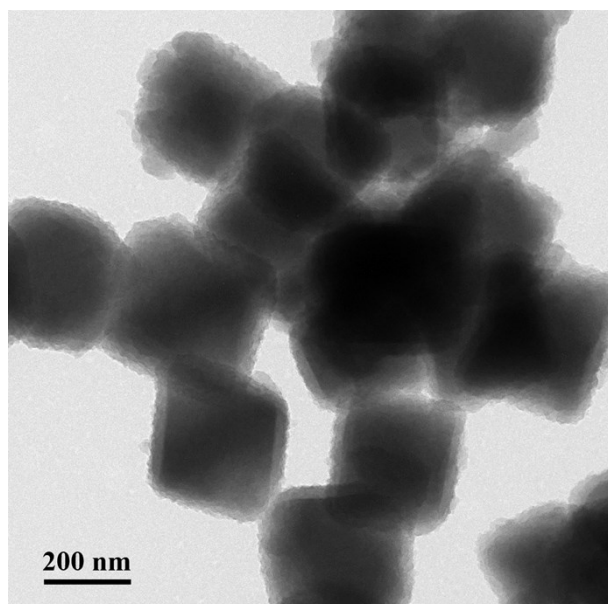


Fig. S15 The TEM image of MOF@TpPa-1-COF.

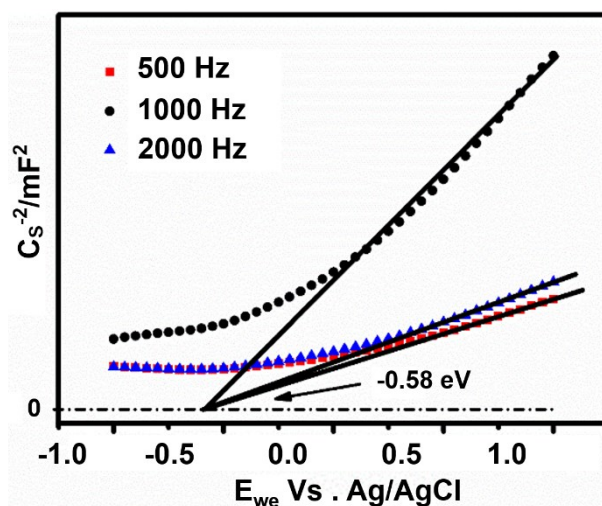


Fig. S16 Different frequency conditions Mott-Schottky curve of MOF-808.

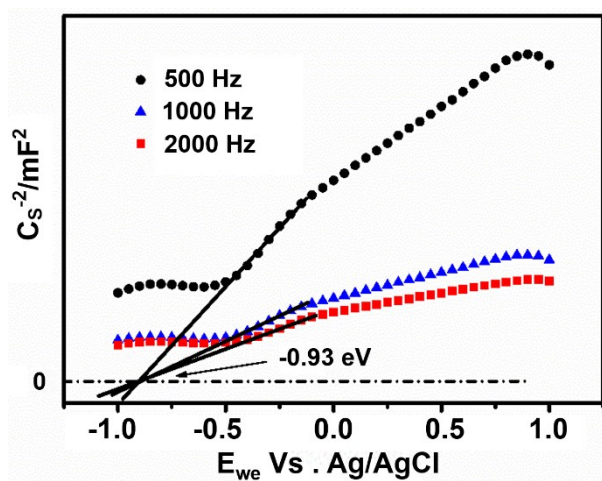


Fig. S17 Different frequency conditions Mott-Schottky curve of TpPa-1-COF.

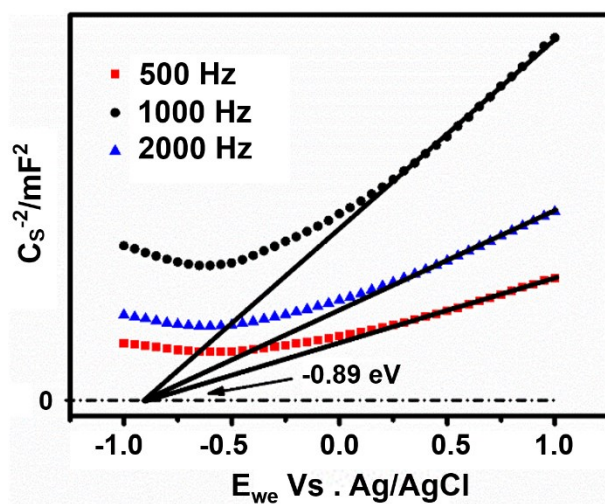


Fig. S18 Different frequency conditions M-S curve of MOF-808@TpPa-1-COF (6:4).

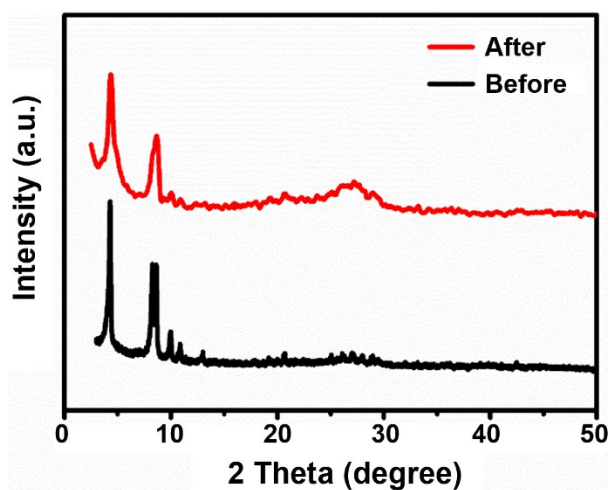


Fig. S19 PXRD patterns of MOF-808@TpPa-1-COF (6:4) hybrid material before and after photocatalysis.

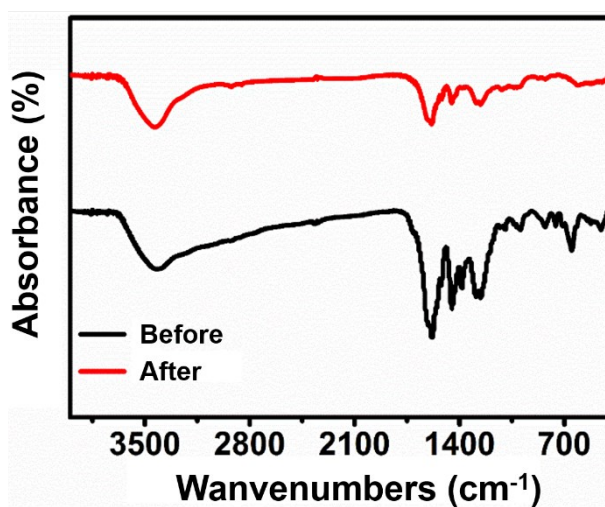


Fig. S20 FT-IR spectra of MOF-808@TpPa-1-COF (6:4) hybrid material before and after photocatalysis.

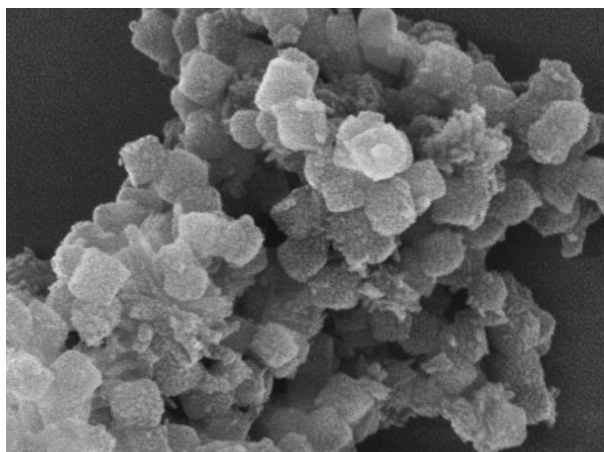


Fig. S21 SEM image of MOF-808@TpPa-1-COF (6:4) hybrid material after photocatalysis.

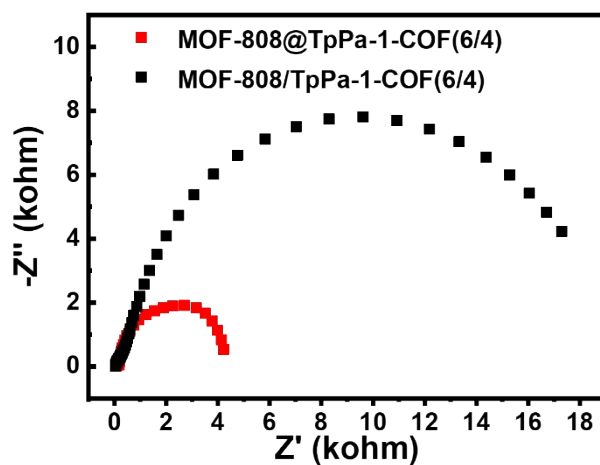


Fig. S22 EIS Nyquist plots of MOF-808@TpPa-1-COF (6/4) and MOF-808/TpPa-1-COF (6/4).

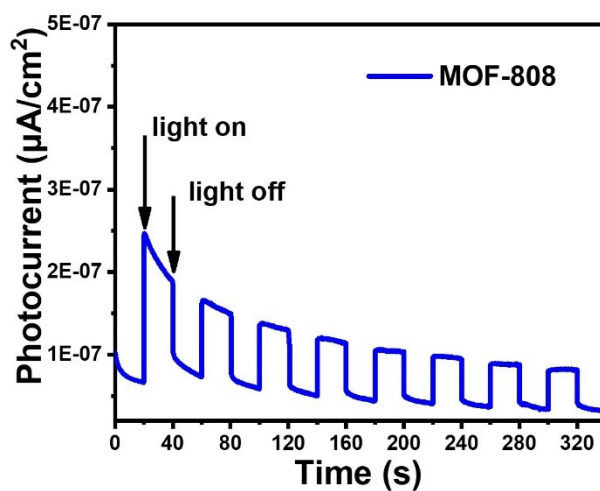


Fig. S23 Transient photocurrents measurements of MOF-808.

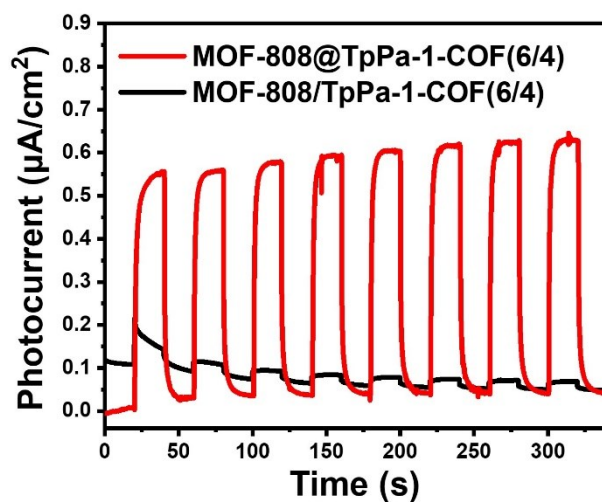


Fig. S24 Transient photocurrents measurements of MOF-808@TpPa-1-COF (6/4) and MOF-808/TpPa-1-COF (6/4).

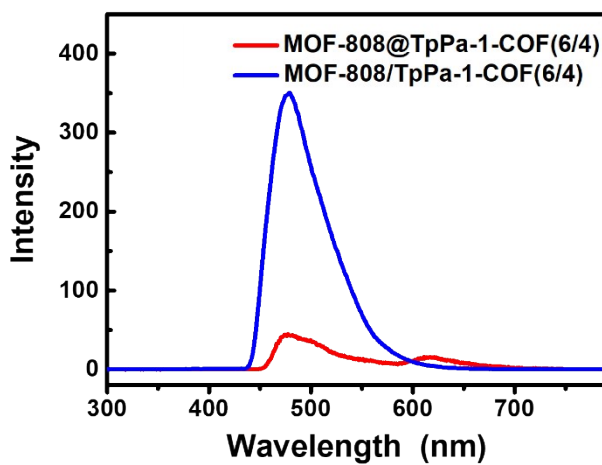


Fig. S25 Photoluminescence spectra MOF-808@TpPa-1-COF (6/4) and MOF-808/TpPa-1-COF (6/4).

Table S2. Summary of some photocatalytic hydrogen evolution based on COFs or MOFs

Catalyst	Cocatalyst	Sacrificial agent	Light source	Activity ($\mu\text{mol}\cdot\text{g}^{-1}\cdot\text{h}^{-1}$)	Ref.
MOF-808@TpPa-1-COF(6/4)	Pt	SA	$\lambda\geq 420$ nm	11880	This work
MOF-808	Pt	TEOA	Full spectrum	1.7	2
U@TDE4	Pt	SA	$\lambda\geq 420$ nm	7178	3
NH ₂ -MIL-125/B-CTF-1	Pt	TEOA	$\lambda\geq 420$ nm	360	4
TpPa-COF-(CH ₃) ₂	Pt	SA	$\lambda\geq 420$ nm	8330	5
TpPa-2-COF/Ni(OH) ₂	Pt	SA	$\lambda\geq 420$ nm	1896	6
MoS ₂ /TpPa-1-COF	Pt	SA	$\lambda\geq 420$ nm	5580	7
CTF-BT/Th-1	Pt	TEOA	$\lambda\geq 420$ nm	6600	8
THA-COF	Pt	TEOA	$\lambda\geq 420$ nm	80	9
N ₃ -COF	Pt	TEOA	$\lambda\geq 420$ nm	1703	10
NUS-55/[Co-(bpy) ₃]Cl ₂	Pt	TEA	$\lambda\geq 420$ nm	2480	11
A-TEBPY-COF	Pt	TEOA	AM 1.5	98	12
ZnPor-DETH-COF	Pt	TEOA	$\lambda\geq 400$ nm	413	13
PyTz-COF	Pt	SA	AM 1.5	2072.4	14
P-COF-1/CTF	Pt	TEOA	$\lambda\geq 420$ nm	14100	15

Reference

- 1 J. H. Chong, M. Sauer, B. O. Patrick and M. J. MacLachlan, *Org. Lett.*, 2003, **5**, 3823-3826.
- 2 H. Liu, C. Y. Xu, D. D. Li and H. L. Jiang, *Angew. Chem., Int. Ed.*, 2018, **57**, 5379-5383.
- 3 Y. Chen, D. Yang, B. Shi, W. Dai, H. Ren, K. An, Z. Zhou, Z. Zhao, W. Wang and Z. Jiang, *J. Mater. Chem. A*, 2020, **8**, 7724-7732.
- 4 F. Li, D. K. Wang, Q. J. Xing, G. Zhou, S. S. Liu, Y. Li, L. L. Zheng, P. Ye and J. P. Zou, *Appl. Catal., B*, 2019, **243**, 621-628.
- 5 J. L. Sheng, H. Dong, X. B. Meng, H. L. Tang, Y. H. Yao, D. Q. Liu, L. L. Bai, F. M. Zhang, J. Z. Wei and X. J. Sun, *Chemcatchem*, 2019, **11**, 2313-2319.
- 6 H. Dong, X. B. Meng, X. Zhang, H. L. Tang, J. W. Liu, J. H. Wang, J. Z. Wei, F. M. Zhang, L. L. Bai and X. J. Sun, *Chem. Eng. J.*, 2020, **379**, 122342.
- 7 M. Y. Gao, C. C. Li, H. L. Tang, X. J. Sun, H. Dong and F. M. Zhang, *J. Mater. Chem. A*, 2019, **7**, 20193-20200.
- 8 W. Huang, Q. He, Y. Hu and Y. Li, *Angew. Chem., Int. Ed.*, 2019, **58**, 8676-8680.
- 9 C. Liu, Y. Xiao, Q. Yang, Y. Wang, R. Lu, Y. Chen, C. Wang and H. Yan, *Appl. Surf. Sci.*, 2021, **537**, 148082.
- 10 V. S. Vyas, F. Haase, L. Stegbauer, G. Savasci, F. Podjaski, C. Ochsenfeld and B. V. Lotsch, *Nat. Commun.*, 2015, **6**, 8508
- 11 J. Wang, J. Zhang, S. B. Peh, G. Liu, T. Kundu, J. Dong, Y. Ying, Y. Qian and D. Zhao, *Sci. China Chem.*, 2020, **63**, 192-197.
- 12 L. Stegbauer, S. Zech, G. Savasci, T. Banerjee, F. Podjaski, K. Schwinghammer, C. Ochsenfeld and B. V. Lotsch, *Adv. Energy. Mater.*, 2018, **8**, 1703278.
- 13 R. Chen, Y. Wang, Y. Ma, A. Mal, X.Y. Gao, L. Gao, L. Qiao, X. B. Li, L. Z. Wu and C. Wang, *Nat. Commun.*, 2021, **12**, 1354.
- 14 W. Li, X. Huang, T. Zeng, Y. A. Liu, W. Hu, H. Yang, Y. B. Zhang and K. Wen, *Angew. Chem., Int. Ed.*, 2021, **60**, 1869-1874.
- 15 N. Xu, Y. Liu, W. Yang, J. Tang, B. Cai, Q. Li, J. Sun, K. Wang, B. Xu, Q. Zhang and Y. Fan, *Acs Applied Energy Materials*, 2020, **3**, 11939-11946.